Optimizing Offsets in Signalized Traffic Networks: A Case Study

Zahra Amini[1] Samuel Coogan[2] Christopher Flores[3] Alexander Skabardonis[4] and Pravin Varaiya[5]

***Abstract*— We evaluate the performance of an algorithm, developed by [1], that formulates offset optimization for a traffic network with arbitrary topology as a quadratically constrained quadratic program. The algorithm adjusts the offset values of traffic signals in urban networks to reduce delay and the number of stops. The performance of two real-world networks using the offsets obtained by the algorithm and those obtained using Synchro, a popular software package for traffic signal timing, is compared via simulation using the VISSIM microscopic traffic simulator. The offsets obtained by the algorithm reduce the average number of stops and total delay that vehicles experience along the major routes in both networks and under several traffic profiles as compared with offsets obtained from Synchro. In addition, the original model assumed infinite storage capacity for links, we eliminate this assumption to make the model more realistic. In this paper we show theoretical work of adding storage capacity constrains to the original optimization problem, along with an example of the results from modified version of the algorithm.**

I. Introduction

Traffic signal offsets specify the timing of a traffic light relative to adjacent signals. Offsets constitute the main parameter for coordinated traffic movement among multiple traffic signals.

Optimizing the offsets in an urban network reduces the delay and the number of stops that vehicles experience. Existing offset optimization algorithms focus on two-way arterial roads. The papers [2] and [3] present algorithms for maximizing the green bandwidth, that is, the length of the time window in which a vehicle can travel along the entire road without being stopped by a red light. Traffic control software such as Synchro [4], TRANSYT [5], [6] optimize offset values by minimizing delay and number of the stops. Recently, advances in data collection technology led to methods for offset optimization using archived traffic data [7].

All of the above-cited methods assume sufficient storage capacity for links and therefore do not consider the risk of *spill-back* in which a segment of road between traffic lights is completely filled with vehicles so that upstream traffic cannot enter the link, even with a green light. However, spill-back is a critical condition that can arise in an urban network; [8] and [9] focus on detecting and modeling spill-back. In some cases spill-back can be prevented by changing the control system setting [10]; another study [11] shows that severe congestion could be improved by dynamically adapting offset values.

The paper [1] introduced a new approach that formulates offset optimization as a quadratically constrained quadratic program amenable to convex relaxation. This approach has many advantages over previous studies. It considers all links in a network with arbitrary topology and is not restricted to a single arterial. Further, the approach is computationally efficient and used in [12] to optimize offsets for large networks with high traffic demand from multiple directions.

We evaluate the performance of the algorithm on two real-world case study networks. These two networks are also simulated using VISSIM microscopic traffic simulator, which simulates traffic patterns realistically [13]. The first network is a ten-intersection portion of the San Pablo Ave. arterial in Berkeley, California, and the second network is a seven-intersection portion of Montrose Rd. and adjacent streets in Montgomery County, Maryland. Under several realistic traffic profiles based on sensor measurement data from the networks, the proposed offset optimization algorithm exhibits better performance compared to the offsets obtained using the Synchro offset optimization tool.

Next, we extend the algorithm in [1] to allow for links with finite storage capacity. By eliminating the assumption of infinite storage capacity we get one step closer to improve the original model and make it more realistic. Moreover, with an example, we show how the result changes when the storage capacity constraints are active.

The rest of the paper is organized as follows. Section II briefly describes the vehicles arrival and departure model and offset optimization algorithm from [1]. Section III presents the simulation results from two different networks. Section IV introduces the storage capacity constraints and extends the algorithm from Section II. Section V presents the evaluation process of the optimization problem when the storage capacity constraints are active with an example, and Section VI explains the conclusions.

II. Algorithm Description

A. Cost Function Formulation

In this section, we briefly recall the traffic network model proposed in [1]. Consider a network with a set $\mathcal{S}$ of signalized intersections and a set $\mathcal{L}$ of *links*. Let $\sigma(l)$ denote the traffic signal at the head of the link l controlling the departure of vehicles from link l, and let $\tau(l)$ denote the signal at the tail of the link l controlling the arrivals of vehicles into link l. (Traffic in a link flows from its tail to its head.)

[1]Civil and Environmental Engineering Department, University of California,Berkeley, zahraamini@berkeley.edu

[2]School of Electrical and Computer Engineering and School of Civil and Environmental Engineering, Georgia Institute of Technology, sam.coogan@gatech.edu

[3]Sensys Networks Inc., Berkeley, CA, 94710, chrisf@sensysnetworks.com

[4]Civil and Environmental Engineering Department, University of California, Berkeley, skabardonis@ce.berkeley.edu

[5]Electrical Engineering Department, University of California, Berkeley, araiya@eecs.berkeley.edu

All signals have a common cycle time T, hence a common frequency $\omega = 2\pi/T$ rad/sec. The signals follow a fixed-time control. Relative to some global clock, each signal s has an offset value of $\theta_s \in [0, 2\pi)$ radians that represents the start time of the fixed control pattern of the intersection. This pattern has designated green interval for each movement that repeats every cycle and controls the vehicle flow. Therefore, each link $l \in \mathcal{L}$ has a queue of length $q_l(t) \geq 0$ at time t equal to the difference between the cumulative arrivals of vehicles, a_l, and departures, d_l,

$$\dot{q}_l(t) = a_l(t) - d_l(t). \tag{1}$$

Note that the queue $q_l(t)$ is the number of vehicles occupying link l at time t, and should not be confused with the (smaller) number of vehicles waiting at intersection $\tau(l)$.

If exogenous arrivals into the network are periodic with period T and there is no spill-back, it is reasonable to assume the network is in periodic steady state so that all arrivals, departures, and queues are also periodic with period T [14].

We then approximate the arrival and departure processes in a link as sinusoids of appropriate amplitude and phase shift. To this end, for each entry link l, the arrival of vehicles into link l at signal $\sigma(l)$ is approximated as

$$\hat{a}_l(t) = A_l + \alpha_l \cos(\omega t - \varphi_l), \tag{2}$$

for constants $A_l, \alpha_l, \varphi_l \geq 0$ with $A_l \geq \alpha_l$. The constant A_l is the average arrival rate of vehicles into link l; α_l allows for periodic fluctuation in the arrival rate.

For a non-entry link l, the arrival process is approximated by

$$\begin{aligned}\hat{a}_l(t) &= \sum_{i\in\mathcal{L}} \beta_{il} A_i (1 + \cos(\omega t - (\theta_{\sigma(i)} + \gamma_i) - \lambda_l)) \\ &= A_l + \alpha_l \cos(\omega t - (\theta_{\tau(l)} + \varphi_l)),\end{aligned} \tag{3}$$

where λ_l denotes the travel time, in radians, of link l and β_{il} denotes the fraction of vehicles that are routed to link l upon exiting link i, which is given and fixed. The mid-point of the green interval in every cycle is specified by its offset $\gamma_i \in [0, 2\pi]$. The signal offsets at the tail and head of each link are respectively θ_τ and θ_σ.

In addition, A_l, α_l, and φ_l are given by

$$A_l = \sum_{i\in\mathcal{L}} \beta_{li} A_i, \tag{4}$$

$$\alpha_l^2 = \left(\sum_{i\in\mathcal{L}} \beta_{il} A_i \cos(\gamma_i)\right)^2 + \left(\sum_{i\in\mathcal{L}} \beta_{il} A_i \sin(\gamma_i)\right)^2, \tag{5}$$

$$\varphi_l = \lambda_l + \arctan\left(\frac{\sum_{i\in\mathcal{L}} \beta_{il} A_k \sin(\gamma_i)}{\sum_{i\in\mathcal{L}} \beta_{il} A_i \cos(\gamma_i)}\right). \tag{6}$$

Similarly, we approximate the departure process for both entry and non-entry links by

$$\hat{d}_l(t) = A_l\big(1 + \cos(\omega t - (\theta_{\sigma(l)} + \gamma_l))\big) \quad \forall l \in \mathcal{L}, \tag{7}$$

where $(\theta_{\sigma(l)} + \gamma_l)$ is the actuation offset of link l as determined by the offset of signal $\sigma(l)$ at the head of link l and the green interval offset, γ_l, of link l.

From equation (1), (3), and (7) we formulate the approximating queueing process, $\hat{q}(t)$, as

$$\begin{aligned}\dot{\hat{q}}_l(t) =& \hat{a}_l(t) - \hat{d}_l(t) \\ =& \alpha_l \cos(\omega t - (\theta_{\tau(l)} + \varphi_l)) \\ & - A_l \cos(\omega t - (\theta_{\sigma(l)} + \gamma_l)) \\ =& Q_l \cos(\omega t - \xi_l),\end{aligned} \tag{8}$$

where

$$Q_l = \sqrt{A_l^2 + \alpha_l^2 - 2A_l\alpha_l \cos((\theta_{\tau(l)} + \varphi_l) - (\theta_{\sigma(l)} + \gamma_l))}, \tag{9}$$

and ξ_l is a phase shift; we omit the explicit expression for ξ_l but note that it is easily computed.

It therefore follows that

$$\hat{q}_l(t) = \frac{Q_l}{\omega} \sin(\omega t - \xi_l) + B_l, \tag{10}$$

where B_l is the average queue length on link l. Since $\hat{q}_l(t)$ cannot be negative, we conclude that $\frac{Q_l}{\omega} \leq B_l$.

The cost function is to minimize the total average queue length in all links, $\sum_{l\in\mathcal{L}} Q_l$. Since the first part $A_l^2 + \alpha_l^2$ of formula (9) is constant, instead of minimizing $\sum_{l\in\mathcal{L}} Q_l$, we can maximize the negative part of the formula, $A_l\alpha_l \cos(\theta_{\tau(l)} - \theta_{\sigma(l)} + \varphi_l - \gamma_l)$ for all links and our objective function becomes

$$\underset{\{\theta_s\}_{s\in\mathcal{S}}}{\text{maximize}} \sum_{l\in\mathcal{L}} A_l\alpha_l \cos(\theta_{\tau(l)} - \theta_{\sigma(l)} + \varphi_l - \gamma_l), \tag{11}$$

in which the offset values, θ_s, are the only decision variables and all other parameters are given by the green splits.

B. Equivalent Quadratically Constrained Quadratic Program (QCQP)

Problem (11) is non-convex. To solve it, [1] uses semi-definite relaxation. To this end, [1] first formulates the equivalent QCQP by defining $z = (x, y)$, where $x_s = \cos(\theta_s)$ and $y_s = \sin(\theta_s)$. Thus, the equivalent cost function becomes $z^T W z$, where

$$W_1[s,u] = \sum_{l\in\mathcal{L}_{s\to u}} A_l\alpha_l \cos(\varphi_l - \gamma_l) \tag{12}$$

$$W_2[s,u] = \sum_{l\in\mathcal{L}_{s\to u}} A_l\alpha_l \sin(\varphi_l - \gamma_l) \tag{13}$$

and

$$\underline{W} = \begin{bmatrix} W_1 & W_2 \\ -W_2 & W_1 \end{bmatrix}, \quad W = \frac{1}{2}(\underline{W} + \underline{W}^T). \tag{14}$$

Also, we have the constraints $x_s^2 + y_s^2 = 1$ for all $s \in \mathcal{S}$. Let $E_s \in \mathbb{R}^{|\mathcal{S}|+1}$ for $s \in \mathcal{S}$ be given by

$$E_s[u,v] = \begin{cases} 1 & \text{if } u = v = s \\ 0 & \text{otherwise} \end{cases} \tag{15}$$

and define

$$M_s = \begin{bmatrix} E_s & 0 \\ 0 & E_s \end{bmatrix}. \tag{16}$$

Then the constraints $x_s^2 + y_s^2 = 1$ are equivalent to $z^T M_s z = 1$. As a result, the optimization problem is

$$\begin{aligned} \underset{z \in \mathbb{R}^{2|S|+2}}{\text{maximize}} \quad & z^T W z \\ \text{subject to} \quad & z^T M_s z = 1 \quad \forall s \in \mathcal{S}. \end{aligned} \tag{17}$$

C. Semi-Definite Program (SDP) Relaxation

The quadratic terms in (17) are of the form $z^T Q z = Tr(QZ)$ with $Z = zz^T$. Further if the matrix Z is positive semi-definite and of rank 1, it can be decomposed as $Z = zz^T$. The advantage of this transformation is that $Tr(QZ)$ is linear in the new variable Z.

In the original offset optimization algorithm, [1] relaxes the exact, non-convex QCQP into a convex Semi-Definite Programming (SDP) by removing the rank constraint and gets the following formulation

$$\begin{aligned} \underset{Z \in \mathbb{R}^{(2|\mathcal{S}|+2)\times(2|\mathcal{S}|+2)}}{\text{maximize}} \quad & \mathbf{Tr}(WZ) \\ \text{subject to} \quad & \mathbf{Tr}(M_s Z) = 1 \quad \forall s \in \mathcal{S} \cup \epsilon \\ & Z \succeq 0. \end{aligned} \tag{18}$$

The solution to the relaxed convex SDP problem gives an upper bound on the value of the optimization problem. This upper bound is the optimum solution of the rank-constrained SDP problem if the solution matrix has rank 1. If solution matrix has rank bigger than 1, [1] proposes vector decomposition as one of the options for obtaining the optimum solution. In this paper, we used vector decomposition to estimate the optimum solution as well.

III. Case Study Networks

A. Sites Description

In this section, we test the performance of the offset optimization algorithm that was developed in [1] on two real world case study networks. Figure 1 shows a ten-intersection portion of San Pablo Ave. in Berkeley, California that serves as our first case study. The figure also indicates the input approaches that have the most traffic volume.

The second case study network is shown in Figure 2, which is a seven-intersection portion of Montrose Rd. in Montgomery County, Maryland. Similar to the first network, Figure 2 indicates the major inputs of the network. This network is equipped with detectors from Sensys Network Inc., a company specializing in wireless traffic detection. According to the detection data, major traffic flows into the network from three directions. The same figure indicates that most traffic in the eastbound direction comes from input 1 and in the westbound direction comes from inputs 2 and 3.

B. Experiment Design for Case Study Networks

We used Synchro 9 to build a test-bed of the networks and then used Synchro's offset optimization tool to optimize the intersection offsets, while other control parameters such as cycle time, green time, split ratio, and etc. are constant. As

Fig. 1. Case study 1: San Pablo Ave Network in Berkeley, California.

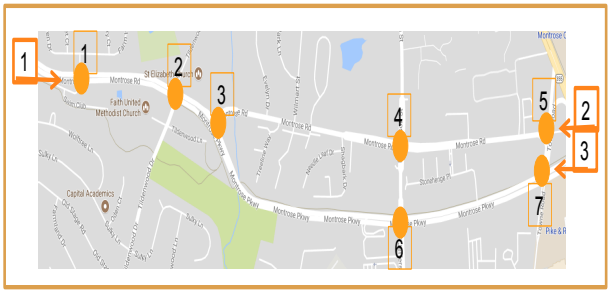

Fig. 2. Case study 2: Montrose Rd. Network in Montgomery County, Maryland.

explained in the Synchro user manual, for each offset combination, Synchro reevaluates the departure patterns at the intersection and surrounding intersections and uses Highway Capacity Manual (HCM) delay equation to recalculate delay values [15]. Then chooses the offset values with the lowest delay as the optimum. We repeated this process for all the traffic profiles and recorded the offset values.

In addition, a simulation test-bed was built in VISSIM 8 for evaluating the performance of different offsets. We used the current signal settings and network information for modeling, and for each traffic profile we tested 2 scenarios:

- Offsets determined by Synchro's optimization method.
- Offsets determined by the proposed offset optimization algorithm.

Based on available data, we designed several different traffic profiles for each network. Figure 3 shows the tested scenarios for the San Pablo Ave Network. For this case study, scenarios 1 and 2 correspond to the traffic during the peak hour in different directions, and scenario 3 corresponds to the traffic during off-peak hours. Figure 4 shows the tested traffic scenarios for the Montrose Rd. Network. For this case, scenarios 1 and 5 represent the AM-peak condition while scenarios 2 and 4 are the PM-peak condition, and scenario 3 represents the mid-day traffic profile.

C. Analysis of the Result for Case Study Networks

For both case study networks and for each traffic scenario, we tested the performance of the offsets suggested by the offset optimization algorithm and offsets suggested by Synchro. To do so, we ran the VISSIM simulation for one hour for each scenario. In order to evaluate the performance

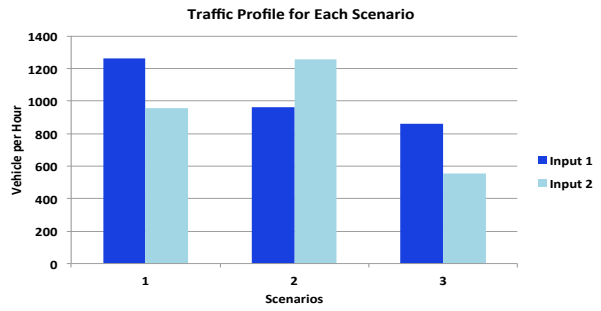

Fig. 3. San Pablo Ave Network traffic profiles

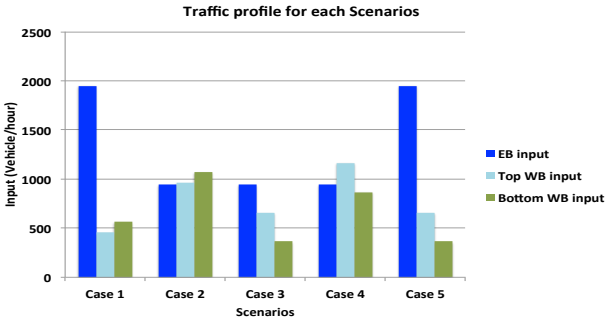

Fig. 4. Montrose Rd. Network traffic profiles

of the network under each offset configuration, we collected the following measures for vehicles moving along the major routes:

- Average number of stops that each vehicle experiences.
- Average vehicle delay that each vehicle experiences.

Major routes have the most traffic volume. In the San Pablo Ave network, these are the south-to-north and north-to-south routes through all intersections. In the Montrose Rd. network, there are four major routes: from west to the upper east leg and vice-versa, and from west to lower east leg and vice-versa.

The following results present the average traffic measures over all the major routes in each network. In Figure 5(a), the orange (respectively, yellow) columns show the average number of the stops that vehicles experience under offset values suggested by Synchro (respectively, the proposed algorithm). Clearly, the algorithm offsets reduce the number of the stops in all three traffic profiles for the San Pablo Ave Network, and up to 20% improvement in scenario 2.

In the Montrose Rd. Network, we tested 5 traffic profiles. Figure 5(b) shows the average number of the stops for these profiles. In all scenarios, the proposed algorithm outperforms Synchro. Scenario 2 shows the most improvement of 30% reduction in the number of stops.

In addition to the number of stops, VISSIM estimates the vehicle delay as the difference between the travel time in free flow condition and actual travel time of each vehicle. This delay includes the time that a vehicle is stopped at red lights and accounts for the acceleration and deceleration time as

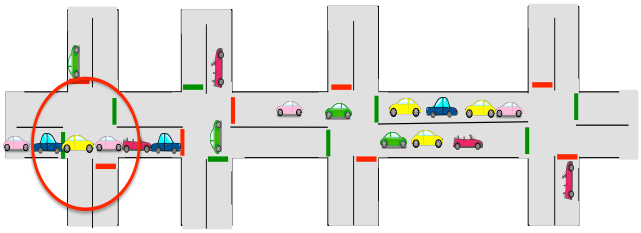

Fig. 6. Queue spill-back at the first intersection (red circle) blocks the entrance.

well. Figure 5(c) shows the average delay for the San Pablo Ave network and we see that for scenario 2, the average delay is reduced, but in scenarios 1 and 3, the average delay remains almost the same. However, in these scenarios, the average number of stops is reduced, as has already been noted in Figure 5(a).

In the Montrose Rd. network, as seen in Figure 5(d), the average delay is lower for all traffic scenarios under offset values suggested by the proposed offset optimization algorithm compared with Synchro, and scenario 2 experiences the most improvement, with 30% reduction in delay.

IV. Storage Capacity Constraints

The result from case studies show the algorithm's suggested offset values improve the traffic condition in the networks. However, this algorithm implicitly assumes infinite storage capacity on links. While this assumption may be sometimes reasonable, as in the case studies above, some networks with short links or high traffic volumes may be susceptible to the spill-back phenomenon where a link exceeds its capacity and the queue blocks upstream traffic flow. In the next two sections we show how to modify the algorithm to work for networks with limited storage capacity links.

A. Storage Capacity Constraint Formulation

At this point we have a model of the average queue length, equation (9), in each link as a function of the offsets θ_s for $s \in \mathcal{S}$. However, in reality, the length of a queue in each link cannot exceed the storage capacity of that link, and if the queue length reaches this capacity, vehicles will not be able to enter the link and will block the upstream intersection; this situation is called *spill-back*. Figure 6 shows an example of the spill-back in a network. The intersection marked by the red circle is experiencing spill-back, and vehicles cannot enter the intersection even though the light is green.

In order to prevent spill-back, we constrain the maximum queue length that can exist in each link, $2B_l$, to be equal or less than the maximum number of the vehicles that can be stored in the link under jam density, k_l. From Section II-A we have $\frac{Q_l}{\omega} \leq B_l$, so for each link $l \in \mathcal{L}$, we introduce the storage capacity constraint

$$\begin{aligned} 2Q_l &\leq \omega k_l \\ \iff Q_l^2 - \left(\frac{\omega k_l}{2}\right)^2 &\leq 0. \end{aligned} \tag{19}$$

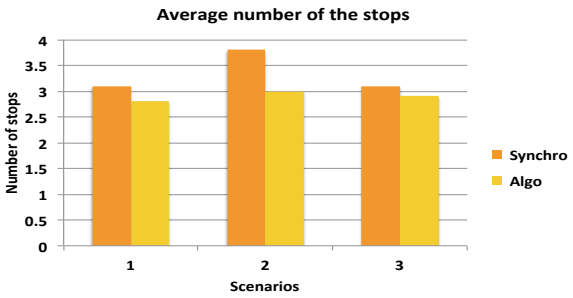

(a) Average number of stops that vehicles experience in San Pablo Ave Network

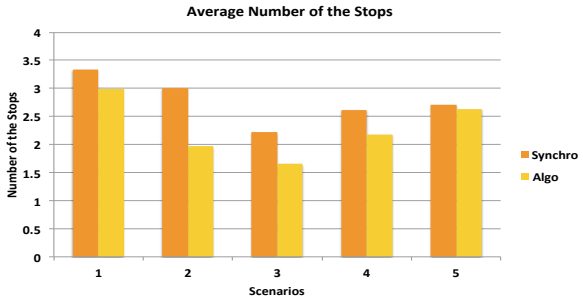

(b) Average number of stops that vehicles experience in Montrose Rd. network

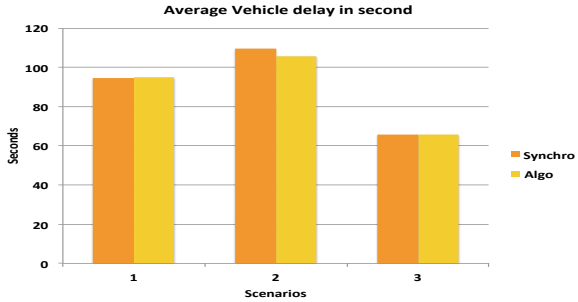

(c) Average vehicle delay in San Pablo Ave Network

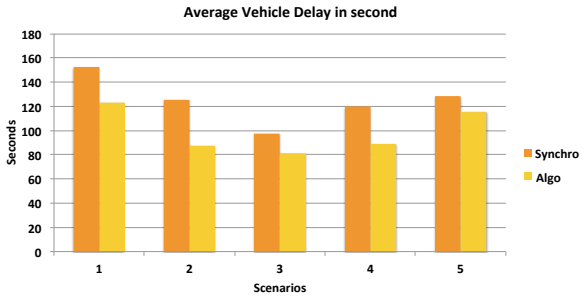

(d) Average vehicle delay in Montrose Rd. Network

Fig. 5. Case studies average vehicle delay and number of the stops results for every scenario

This leads to the final optimization problem by adding the constraint (19) to (11)

$$\begin{aligned} \underset{\{\theta_s\}_{s\in\mathcal{S}}}{\text{maximize}} \quad & \sum_{l\in\mathcal{L}} A_l\alpha_l\cos(\theta_{\tau(l)}-\theta_{\sigma(l)}+\varphi_l-\gamma_l) \\ \text{subject to} \quad & Q_l^2-\left(\frac{\omega k_l}{2}\right)^2\le 0 \quad \forall l\in\mathcal{L}. \end{aligned} \tag{20}$$

B. Solving the Optimization Problem

In Subsection IV-A, we introduced the concept of storage capacity constraints that would protect the network against suffering from spill-back. Now, to incorporate these constraints in the QCQP formulation, for each link we have $z^TC_lz \le K_l$ where $K_l = -A_l^2-\alpha_l^2+(\frac{\omega k_l}{2})^2$ and C_l is given by

$$C_{1[s,u]} = \begin{cases} -2A_l\alpha_l\cos(\varphi_l-\gamma_l) & \text{if } s=\tau(l) \text{ and } u=\sigma(l) \\ 0 & \text{otherwise} \end{cases}$$

$$C_{2[s,u]} = \begin{cases} -2A_l\alpha_l\sin(\varphi_l-\gamma_l) & \text{if } s=\tau(l) \text{ and } u=\sigma(l) \\ 0 & \text{otherwise} \end{cases}$$

with

$$\underline{C_l} = \begin{bmatrix} C_1 & C_2 \\ -C_2 & C_1 \end{bmatrix}, \quad C_l = \frac{1}{2}(\underline{C_l}+\underline{C_l}^T). \tag{21}$$

The original optimization problem from (17) together with the new storage capacity constraints leads to

$$\begin{aligned} \underset{z\in\mathbb{R}^{2|\mathcal{S}|+2}}{\text{maximize}} \quad & z^TWz \\ \text{subject to} \quad & z^TM_sz=1 \quad \forall s\in\mathcal{S} \\ & z^TC_lz\le K_l \quad \forall l\in\mathcal{L}. \end{aligned} \tag{22}$$

Then, we relax the exact, non- convex QCQP into a convex Semi-Definite Programming (SDP) by removing the rank constraint

$$\begin{aligned} \underset{Z\in\mathbb{R}^{(2|\mathcal{S}|+2)\times(2|\mathcal{S}|+2)}}{\text{maximize}} \quad & \mathbf{Tr}(WZ) \\ \text{subject to} \quad & \mathbf{Tr}(M_sZ)=1 \quad \forall s\in\mathcal{S}\cup\epsilon \\ & \mathbf{Tr}(C_lZ)\le K_l \quad \forall l\in\mathcal{L} \\ & Z\succeq 0. \end{aligned} \tag{23}$$

If Z has rank higher than 1, we use vector decomposition to estimate the result.

V. Algorithm Evaluation

A. New Algorithm's Evaluation

Now, let's test the algorithm by assuming a network such as the one in Figure 6, with 4 intersections and fixed common cycle time for all intersections. Starting from the most left hand side intersection, we have intersection 1, 2, 3, and 4. Also, there is link 1, connecting intersection 1 and 2, link 2, connecting intersection 2 and 3, and finally we have link 3, connecting intersection 3 and 4.

Input demand from minor streets to the network is minimal and there are 800 and 500 vehicle per hour traffic flow on the eastbound and westbound approaches. We assumed a fixed predesigned timing plan for signals but used the Offset Optimization Algorithm to estimate the offset values under the following condition

- **Scenario 1**: Infinite storage capacities for links.
- **Scenario 2**: Storage capacity of link 1, 2, and 3 are respectively 3, 4, and 5 vehicles.

Intersection	1	2	3	4
Offset values in seconds for scenario 1	0	4	10	19
Offset values in seconds for scenario 2	0	3	7	12

TABLE I

OFFSET VALUE OF EACH INTERSECTION UNDER THE TWO SCENARIOS

Link	Number of vehicles in Scenario 1	Number of vehicles in Scenario 2
Link 1 EB	1.8	2.2
Link 2 EB	2.3	3.0
Link 3 EB	2.5	4.6
Link 1 WB	3.2	3.0
Link 2 WB	4.4	4.0
Link 3 WB	6.0	5.0

TABLE II

MAXIMUM NUMBER OF VEHICLES IN QUEUE UNDER THE TWO SCENARIOS

As a result, Table I shows the offset values before and after applying the storage capacity constraints on the links. Moreover, Table II presents the algorithm's estimated values of the maximum number of the vehicles in the queue in each link under each scenario. According to that table, the maximum queue length in link 1 WB, 2 WB, and 3 WB are smaller in scenario 2 and they are equal to the storage capacity values of the links. However, the maximum queue length in link 1 EB, 2 EB, and 3 EB, increase due to the new offset values.

With the current model, estimated queue length values from the algorithm are not equal to the queue length from simulation, because the model does not consider the car following theory. So we will not be able to test the new algorithm in a simulator and on a real world network. But if we improve the model to estimate an accurate queue length value, we can use the storage capacity constraints to prevent spill-back in links.

VI. CONCLUSION

In this paper, we evaluated the performance of an offset optimization algorithm on two real world networks under several traffic profiles. In almost all cases, the offset values obtained by the proposed algorithm reduce the average number of the stops and total delay that vehicles experience as compared to Synchro's extracted optimum offset values. We used Synchro's suggested optimum offset value as our baseline because it is a popular method among transportation engineers that is commonly used in practice.

The improvement varies depending on the geometry of the network and traffic profile. However, in all scenarios, the proposed offset optimization algorithm has better performance compared to Synchro. Networks that are larger and more complicated, in other words having multiple major traffic inputs, such as Montrose Rd. network, are likely to benefit more from the proposed offset optimization method because by considering the demand in all the existing links and traffic approaches, this algorithm can also improve network congestion in a time-efficient manner. For example, in the Montrose Rd. network, the offset optimization algorithm reduces the delay and number of the stops by about 30% in some traffic profiles.

In the last sections of the paper, we extended the original offset optimization algorithm by eliminating the assumption of infinite storage capacities for links. We added storage capacity constraints to the optimization problem, so the maximum queue length in the links can not pass the storage capacity of the links. The ultimate goal is to prevent spill-back in the network by controlling the maximum queue length in critical links. In order to achieve this, we need to improve the current model in a way that it will estimate a more accurate queue length value. One approach for improving the current algorithm in future, is to use multiple sinusoidal waves to model arrival and departure instead of using a single wave.

REFERENCES

[1] S. Coogan, E. Kim, G. Gomes, M. Arcak, and P. Varaiya, "Offset optimization in signalized traffic networks via semidefinite relaxation," *Transportation Research Part B: Methodological*, vol. 100, pp. 82–92, 2017.

[2] J. D. Little, M. D. Kelson, and N. H. Gartner, "Maxband: A versatile program for setting signals on arteries and triangular networks," 1981.

[3] G. Gomes, "Bandwidth maximization using vehicle arrival functions," *IEEE Transactions on Intelligent Transportation Systems*, vol. 16, no. 4, pp. 1977–1988, 2015.

[4] D. Husch and J. Albeck, "Trafficware Synchro 5.0 User Guide for Windows," 2001.

[5] D. I. Robertson, "TRANSYT: A traffic network study tool," *Report LR 253*, 1967.

[6] D. I. Robertson and R. D. Bretherton, "Optimizing networks of traffic signals in real time-the SCOOT method," *IEEE Transactions on Vehicular Technology*, vol. 40, no. 1, pp. 11–15, 1991.

[7] H. Hu and H. X. Liu, "Arterial offset optimization using archived high-resolution traffic signal data," *Transportation Research Part C: Emerging Technologies*, vol. 37, pp. 131–144, 2013.

[8] E. Christofa, J. Argote, and A. Skabardonis, "Arterial queue spillback detection and signal control based on connected vehicle technology," *Transportation Research Record: Journal of the Transportation Research Board*, no. 2356, pp. 61–70, 2013.

[9] G. Gentile, L. Meschini, and N. Papola, "Spillback congestion in dynamic traffic assignment: a macroscopic flow model with time-varying bottlenecks," *Transportation Research Part B: Methodological*, vol. 41, no. 10, pp. 1114–1138, 2007.

[10] G. Abu-Lebdeh and R. Benekohal, "Genetic algorithms for traffic signal control and queue management of oversaturated two-way arterials," *Transportation Research Record: Journal of the Transportation Research Board*, no. 1727, pp. 61–67, 2000.

[11] C. F. Daganzo, L. J. Lehe, and J. Argote-Cabanero, "Adaptive offsets for signalized streets," *Transportation Research Procedia*, vol. 23, pp. 612–623, 2017.

[12] E. S. Kim, C.-J. Wu, R. Horowitz, and M. Arcak, "Offset optimization of signalized intersections via the Burer-Monteiro method," in *American Control Conference (ACC), 2017*. IEEE, 2017, pp. 3554–3559.

[13] A. PTV, "Vissim 5.40 user manual," *Karlsruhe, Germany*, 2011.

[14] A. Muralidharan, R. Pedarsani, and P. Varaiya, "Analysis of fixed-time control," *Transportation Research Part B: Methodological*, vol. 73, pp. 81–90, 2015.

[15] H. C. Manual, "Highway capacity manual," *Washington, DC*, p. 11, 2000.